Available online at www.sciencedirect.com

ScienceDirect

Pattern Recognition 41 (2008) 607–615

PATTERN RECOGNITION
THE JOURNAL OF THE PATTERN RECOGNITION SOCIETY

www.elsevier.com/locate/pr

A new calibration model of camera lens distortion

Jianhua Wang*, Fanhuai Shi, Jing Zhang, Yuncai Liu

Institute of Image Processing and Pattern Recognition, Shanghai Jiao Tong University, 800 Dong Chuan Road, Shanghai 200240, PR China

Received 28 April 2006; received in revised form 9 February 2007; accepted 28 June 2007

Abstract

Lens distortion is one of the main factors affecting camera calibration. In this paper, a new model of camera lens distortion is presented, according to which lens distortion is governed by the coefficients of radial distortion and a transform from ideal image plane to real sensor array plane. The transform is determined by two angular parameters describing the pose of the real sensor array plane with respect to the ideal image plane and two linear parameters locating the real sensor array with respect to the optical axis. Experiments show that the new model has about the same correcting effect upon lens distortion as the conventional model including all the radial distortion, decentering distortion and prism distortion. Compared with the conventional model, the new model has fewer parameters to be calibrated and more explicit physical meaning.

Keywords: Camera calibration; Lens distortion; Image correction

1. Introduction

Camera calibration has always been an important issue in photogrammetry and computer vision. Up to now, a variety of methods, see Refs. [1–10] to cite a few, have been developed to accommodate various applications. Theoretically these methods can solve almost all problems about camera calibration. However, in our practice of designing vision system for surgical robot, we found that camera lens distortion and noise in images are two main factors hindering us from getting good calibration. Here we will focus on lens distortion.

The research on camera lens distortion can be traced back to 1919, when A. Conrady first introduced the decentering distortion model. Based on Conrady's work, in 1966 Brown presented the famous Brown–Conrady model [1,8]. In this model, Brown classified lens distortion into radial distortion and tangential distortion, and proposed the famous plumb line method to calibrate these distortions. Since then Brown–Conrady model has been widely used, see Refs. [3,5,9,11] to cite a few. Some modifications to the model have been reported [12–17], but they are mainly focused on mathematical treatments, lacking physical analysis of the distortion sources and relation among different distortion components. In addition, a general model has been presented in Ref. [18], but it is a conceptual one so far without quantitative evaluation. Recently, a nonparametric radial distortion model has been proposed in Ref. [19], but it considers only radial distortion. Although the radial component of lens distortion is predominant, it is coupled with tangential one. Therefore modeling radial distortion without considering tangential part is not enough. So far the basic formula expressing lens distortion as a sum of radial distortion, decentering distortion and thin prism distortion is still the main stream of distortion models, which is called conventional model in this paper.

According to the conventional model, the decentering distortion is resulted from various decentering and has both radial and tangential components [1,2,5]. Thin prism distortion arises from slight tilt of lens or image sensor array and also causes additional radial and tangential distortion [1,2,5]. Here we can see that the radial distortion, decentering distortion and thin prism distortion are coupled with one another, because both decentering distortion and thin prism distortion have a contribution to radial component. Can we find another way to unify all the three types of distortion?

Now that decentering distortion and thin prism distortion come from decentering and tilt, and decentering and tilt can be described mathematically by a translation vector and a rotation matrix, then we can express them in a transform consisting of

* Corresponding author. Tel.: +86 21 34204028; fax: +86 21 34204340.
E-mail address: jian-hua.wang@sjtu.edu.cn (J. Wang).

0031-3203/$30.00
doi:10.1016/j.patcog.2007.06.012

rotation and translation. Inspired by this idea, we present a new model of lens distortion in this paper.

We start with a brief review of the previous work in Section 2. Then our work is presented in detail, including analysis of lens distortion in Section 3, the new model of lens distortion in Section 4, calibration method of the new model in Section 5, and experiment results and discussions in Section 6. Finally a conclusion is drawn in Section 7.

2. Previous work

Lens distortion can usually be expressed as

$$u_d = u + \delta_u(u, v),$$
$$v_d = v + \delta_v(u, v), \tag{1}$$

where u and v are the unobservable distortion-free image coordinates; u_d and v_d are the corresponding image coordinates with distortion; $\delta_u(u, v)$ and $\delta_v(u, v)$ are distortion in u and v direction respectively, which can be classified into three types: radial distortion, decentering distortion and thin prism distortion.

Radial distortion is caused by flawed radial curvature of a lens and governed by the following equation [5]:

$$\delta_{ur}(u, v) = u(k_1 r^2 + k_2 r^4 + k_3 r^6 + \cdots),$$
$$\delta_{vr}(u, v) = v(k_1 r^2 + k_2 r^4 + k_3 r^6 + \cdots), \tag{2}$$

where k_1, k_2, k_3 are radial distortion coefficients; r is the distance from a point (u, v) to the center of radial distortion. The first and the second terms are predominant, while the other terms are usually negligible. So the radial distortion formula can usually be reduced as

$$\delta_{ur}(u, v) = u(k_1 \cdot r^2 + k_2 \cdot r^4),$$
$$\delta_{vr}(u, v) = v(k_1 \cdot r^2 + k_2 \cdot r^4). \tag{3}$$

Decentering distortion comes from various decentering of lens and other optical components and can be described by the following expressions [5]:

$$\delta_{ud}(u, v) = p_1(3u^2 + v^2) + 2p_2 \cdot u \cdot v,$$
$$\delta_{vd}(u, v) = p_2(3v^2 + u^2) + 2p_1 \cdot u \cdot v, \tag{4}$$

where p_1 and p_2 are coefficients of decentering distortion.

Thin prism distortion arises mainly from tilt of a lens with respect to the image sensor array and can be represented by the following formula [5]:

$$\delta_{up}(u, v) = s_1(u^2 + v^2),$$
$$\delta_{vp}(u, v) = s_2(u^2 + v^2), \tag{5}$$

where s_1 and s_2 are coefficients of thin prism distortion.

Then the total lens distortion of a camera can be expressed as

$$\begin{aligned}\delta_u(u, v) &= k_1 u(u^2 + v^2) + k_2 u(u^2 + v^2)^2 + (p_1(3u^2 + v^2) \\ &\quad + 2p_2 uv) + s_1(u^2 + v^2), \\ \delta_v(u, v) &= k_1 v(u^2 + v^2) + k_2 v(u^2 + v^2)^2 + (p_2(3v^2 + u^2) \\ &\quad + 2p_1 uv) + s_2(u^2 + v^2).\end{aligned} \tag{6}$$

This formula is based on undistorted image coordinates and used in camera calibration. It transforms an undistorted image point (u, v) into a distorted image point (u_d, v_d).

In nonmetric calibration of lens distortion, an inversed formula that transforms a distorted image point (u_d, v_d) into an undistorted image point (u, v) is often used, which can be expressed as [22]

$$u = u_d + \delta_{u_d}(u_d, v_d),$$
$$v = v_d + \delta_{v_d}(u_d, v_d), \tag{7}$$

where

$$\begin{aligned}\delta_{u_d}(u_d, v_d) &= k_1 u_d(u_d^2 + v_d^2) + k_2 u_d(u_d^2 + v_d^2)^2 \\ &\quad + (p_1(3u_d^2 + v_d^2) + 2p_2 u_d v_d) + s_1(u_d^2 + v_d^2), \\ \delta_{v_d}(u_d, v_d) &= k_1 v_d(u_d^2 + v_d^2) + k_2 v_d(u_d^2 + v_d^2)^2 \\ &\quad + (p_2(3v_d^2 + u_d^2) + 2p_1 u_d v_d) + s_2(u_d^2 + v_d^2).\end{aligned} \tag{8}$$

In formulas (6) and (8), the distortion center is the same, but corresponding coefficients of distortion are different. These two formulas are same in form, and they are referred as the conventional models in this paper. Discussions hereinafter are mainly based on formula (6), and all derivations can be adapted to formula (8).

3. Analysis of lens distortion

Formula (4) can be rewritten as

$$\delta_{ud}(u, v) = p_1(u^2 + v^2) + u(2p_1 \cdot u + 2p_2 \cdot v),$$
$$\delta_{vd}(u, v) = p_2(v^2 + u^2) + v(2p_1 \cdot u + 2p_2 \cdot v), \tag{9}$$

then formula (6) can be rewritten as:

$$\begin{aligned}\delta_u(u, v) &= k_1 u(u^2 + v^2) + k_2 u(u^2 + v^2)^2 + (p_1 + s_1) \\ &\quad (u^2 + v^2) + u(2p_1 \cdot u + 2p_2 \cdot v), \\ \delta_v(u, v) &= k_1 v(u^2 + v^2) + k_2 v(u^2 + v^2)^2 + (p_2 + s_2) \\ &\quad (u^2 + v^2) + v(2p_1 \cdot u + 2p_2 \cdot v).\end{aligned} \tag{10}$$

It can be seen from formula (10) that the coefficients of thin prism distortion s_1 and s_2 are coupled with the coefficients of decentering distortion p_1 and p_2 in formula (6). To decouple them, let

$$q_1 = s_1 + p_1,$$
$$q_2 = s_2 + p_2 \tag{11}$$

and replace $2p_1$ and $2p_2$with new p_1 and p_2, respectively, then we obtain the improved lens distortion model:

$$\begin{aligned}\delta_u(u, v) &= k_1 u(u^2 + v^2) + k_2 u(u^2 + v^2)^2 + q_1(u^2 + v^2) \\ &\quad + u(p_1 \cdot u + p_2 \cdot v), \\ \delta_v(u, v) &= k_1 v(u^2 + v^2) + k_2 v(u^2 + v^2)^2 + q_2(u^2 + v^2) \\ &\quad + v(p_1 \cdot u + p_2 \cdot v).\end{aligned} \tag{12}$$

The effects of the coefficients k_1, k_2, q_1, q_2, p_1 and p_2 in formula (12) are shown in Fig. 1. From formula (12) and Fig. 1,

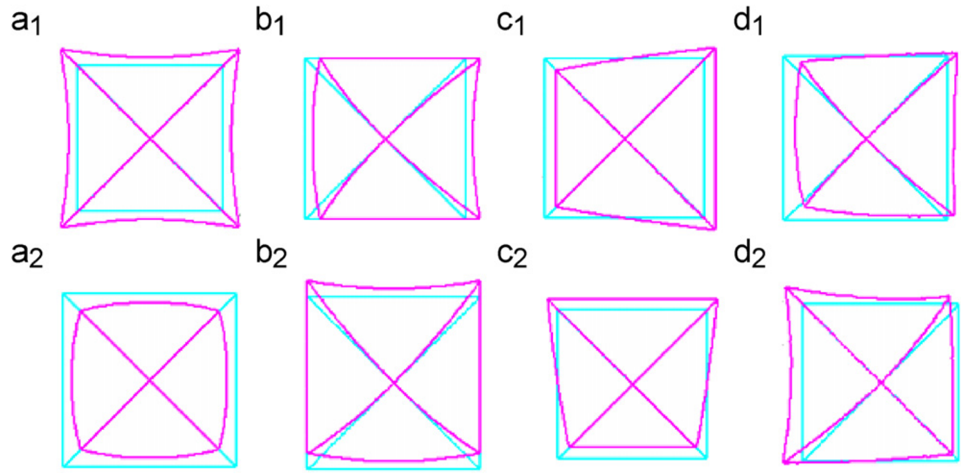

Fig. 1. Effects of the coefficients in the improved lens distortion model. The square in cyan is the distortion-free image. (a_1) and (a_2) show the effects of coefficient k_1, where $k_1 = 3.0 \times 10^{-6}$ for (a_1), and $k_1 = -3.0 \times 10^{-6}$ for (a_2); (b_1) and (b_2) show the effects of coefficients q_1 and q_2, where $q_1 = 5.0 \times 10^{-4}$, $q_2 = 0$ for (b_1), and $q_1 = 0$, $q_2 = -5.0 \times 10^{-4}$ for (b_2); (c_1) and (c_2) show the effects of coefficients p_1 and p_2, where $p_1 = 8.0 \times 10^{-4}$, $p_2 = 0$ for (c_1) and $p_1 = 0$, $p_2 = -8.0 \times 10^{-4}$ for (c_2); (d_1) and (d_2) show the effects of coefficients k_1, p_1, p_2, q_1 and q_2 together, where $k_1 = -1.0 \times 10^{-6}$, $q_1 = 3.0 \times 10^{-4}$, $q_2 = 1.0 \times 10^{-4}$, $p_1 = 3.0 \times 10^{-4}$, $p_2 = 1.0 \times 10^{-4}$ for (d_1), and $k_1 = 1.0 \times 10^{-6}$, $q_1 = -3.0 \times 10^{-4}$, $q_2 = -3.0 \times 10^{-4}$, $p_1 = -3.0 \times 10^{-4}$, $p_2 = 1.0 \times 10^{-4}$ for (d_2).

specifically (b1), (c1), (b2), and (c2), it can be seen that in the improved model, the coefficients k_1,k_2,q_1,q_2,p_1 and p_2 are independent mathematically from one another. However, are they independent from one another physically?

In the conventional model, various sources of lens distortion have been pointed out, but the relation among radial distortion, decentering distortion and thin prism distortion has not been discussed. In other words, radial distortion, decentering distortion and thin prism distortion are treated as being independent from one another. However, they are not independent from one another in fact, as discussed above.

On the one hand, lenses are usually manufactured on precise rotational equipments, and therefore radial symmetry can be ensured. On the other hand, it is hard to avoid the eccentricity and tilt of the optical components with respect to one another in the assembling process of a camera. When the optical axis of a lens is decentered or tilted with respect to image sensor array, the radial distortion will be distorted and the radial symmetry broken. As a result, a part of the radial distortion will manifest itself in the form of decentering distortion or prism distortion. In other words, tangential component of lens distortion comes from distortion of radial distortion in fact. Of course, tangential distortion can also come from asymmetric error arising in the manufacturing process and nonuniformity of lens material, but they are small enough to be neglected in view of optical element manufacturing. Therefore, though the coefficients k_1, k_2, q_1, q_2, p_1 and p_2 in the improved model (12) are independent from one another mathematically, they are not independent from one another physically. The answer hints us the possibility to reduce the improved model further.

Since tangential distortion comes from decentering and tilt, and decentering and tilt can be described mathematically by a translation vector and a rotation matrix. Then we can express tangential distortion with a transform consisting of rotation and translation. In this way, we obtain our new model for calibration of lens distortion.

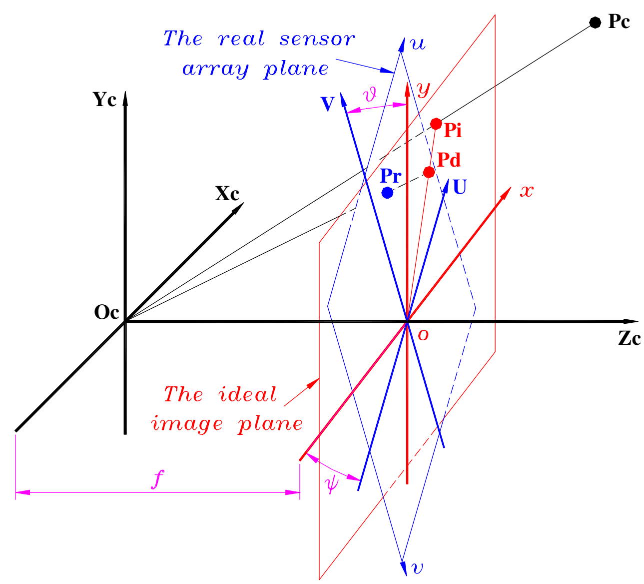

Fig. 2. The imaging model.

4. The new model of lens distortion

Because we focus on lens distortion, without loss of generality, we can suppose a point P_c lies in the camera coordinate system $O_c X_c Y_c Z_c$. According to the new model, the point is imaged onto the real image sensor array in four stages as shown in Fig. 2.

(1) The point $P_c = [X_c \quad Y_c \quad Z_c]^{\mathrm{T}}$ is imaged onto the ideal image plane according to a pinhole camera model without any lens distortion. This stage is a perspective projecting process, which can be expressed as

$$[x \quad y \quad f]^{\mathrm{T}} = \frac{f}{Z_c}[X_c \quad Y_c \quad Z_c]^{\mathrm{T}}, \tag{13}$$

where f is focal length of the lens, (x, y) is the coordinates of the distortion-free image point p_i on the ideal image plane oxy.

(2) The distortion-free image point $p_i = [x \quad y \quad 0]^{\mathrm{T}}$ shifts to $p_d = [x_d \quad y_d \quad 0]^{\mathrm{T}}$ on the ideal image plane oxy due to radial distortion, which can be formulated as

$$\begin{bmatrix} x_d \\ y_d \end{bmatrix} = [1 + k_1(x^2 + y^2) + k_2(x^2 + y^2)^2] \begin{bmatrix} x \\ y \end{bmatrix}, \tag{14}$$

where k_1 and k_2 are the first and the second order radial distortion coefficients, respectively. Here we consider only the first and the second order radial distortion, because they are predominant and in most cases are enough to practical use. If necessary, other higher order terms as in Eq. (2) can be counted in.

(3) The distorted image point $p_d = [x_d \quad y_d \quad 0]^{\mathrm{T}}$ on the ideal image plane coordinate system oxy is transformed to $[x_{di} \quad y_{di} \quad z_{di}]^{\mathrm{T}}$ in the real sensor array plane coordinate system OUV, which can be expressed as

$$[x_{di} \quad y_{di} \quad z_{di}]^{\mathrm{T}} = R_c [x_d \quad y_d \quad 0]^{\mathrm{T}}, \tag{15}$$

where R_c is a rotation matrix from ideal image plane coordinate system oxy to real sensor array plane coordinate system OUV. Due to the real sensor array plane can be located only through two rotation angles around axes x and y, no rotation around axis z is necessary. Suppose the rotation angles around axis x and axis y are θ and ψ, respectively, then R_c can be expressed as

$$R_c = R_\psi \cdot R_\theta, \tag{16}$$

where R_θ and R_ψ are rotation matrix around axis x and axis y, respectively, which can be expressed as

$$R_\theta = \begin{bmatrix} 1 & 0 & 0 \\ 0 & \cos\theta & -\sin\theta \\ 0 & \sin\theta & \cos\theta \end{bmatrix}; \quad R_\psi = \begin{bmatrix} \cos\psi & 0 & \sin\psi \\ 0 & 1 & 0 \\ -\sin\psi & 0 & \cos\psi \end{bmatrix}. \tag{17}$$

Because θ and ψ are very small, R_θ and R_ψ can be reduced as

$$R_\theta = \begin{bmatrix} 1 & 0 & 0 \\ 0 & 1 & -\theta \\ 0 & \theta & 1 \end{bmatrix}; \quad R_\psi = \begin{bmatrix} 1 & 0 & \psi \\ 0 & 1 & 0 \\ -\psi & 0 & 1 \end{bmatrix} \tag{18}$$

and therefore R_c can be reduced as

$$R_c = \begin{bmatrix} 1 & 0 & \psi \\ 0 & 1 & -\theta \\ -\psi & \theta & 1 \end{bmatrix}. \tag{19}$$

The straight line from camera optical center O_c to point $[x_{di} \quad y_{di} \quad z_{di}]^{\mathrm{T}}$ intersects with the real sensor array plane at point $P_r = [U \quad V]^{\mathrm{T}}$, and the intersect point P_r is just the real image point, which can be expressed as

$$U = \frac{x_d \cdot f}{\theta \cdot y_d - \psi \cdot x_d + f}; \quad V = \frac{y_d \cdot f}{\theta \cdot y_d - \psi \cdot x_d + f}. \tag{20}$$

(4) The real image point $P_r = [U \quad V]^{\mathrm{T}}$ in the sensor array plane coordinate system OUV is converted into $[u \quad v]^{\mathrm{T}}$ in the pixel coordinate system according to the sensor unit cell size and the principal point coordinates, which can be formulated as

$$\begin{bmatrix} u \\ v \end{bmatrix} = \begin{bmatrix} \dfrac{1}{\mathrm{d}x} & 0 \\ 0 & \dfrac{1}{\mathrm{d}y} \end{bmatrix} \begin{bmatrix} U \\ V \end{bmatrix} + \begin{bmatrix} u_0 \\ v_0 \end{bmatrix}, \tag{21}$$

where (u_0, v_0) is coordinates of the principal point, which is coincident with the center of distortion [7], $\mathrm{d}x$ and $\mathrm{d}y$ are the unit cell size of the CCD sensor in U and V directions, respectively.

5. Calibration method of the new model

Methods to calibrate parameters of a distortion model fall into two classes, the total calibration [3,5,9] and the nonmetric calibration [11,21,22]. The total calibration methods use a calibration object whose geometrical structure is accurately known. In the total calibration methods, distortion parameters are obtained together with other intrinsic and extrinsic parameters of the camera. Because of coupling between distortion parameters and other intrinsic and extrinsic parameters, sometimes false result may be obtained, which is the disadvantage of the total calibration methods. The nonmetric methods utilize projecting invariants, not relying on any calibration object of known structure. In this class of methods, the most important invariant is straight line. Calibration methods of lens distortion based on straight line rely on the fact that a straight line remains a straight line in perspective projecting process if and only if there is no lens distortion [11]. Straight-line based methods are the main stream in calibration of lens distortion so far. In straight-line based methods, the most widely used distortion measure is the sum of fitting residues. Recently, Ahmed and Farag proposed a new distortion measure, the sum of slope differences between tangents at two neighbor points of a line [22]. When this distortion measure is used, no straight-line fitting is needed.

To validate the new model, we calibrate cameras by two typical straight-line based methods proposed in Refs. [11,22], wherein the method in Ref. [11] is referred as method one and the method in Ref. [22] is referred as method two. When method one is used, the measure of lens distortion is the sum of fitting residues in an image, which is denoted as Re. When method two is used, the measure of lens distortion is sum of slope differences between tangents at two neighbor points of a line in an image, which is denoted as ξs.

To have a comparison, four models of lens distortion are calibrated by these two methods. In model I, only the first order radial distortion coefficient k_1 is considered. Model II includes both the first and the second order radial distortion coefficients k_1 and k_2. Model III is the new model including the first and the second order radial distortion coefficients k_1 and k_2, the pitch angle θ and yaw angle ψ. Model IV is the conventional model including the first and the second order radial distortion coefficients k_1 and k_2, the decentring distortion coefficients p_1, p_2 and the prism distortion coefficients q_1 and q_2.

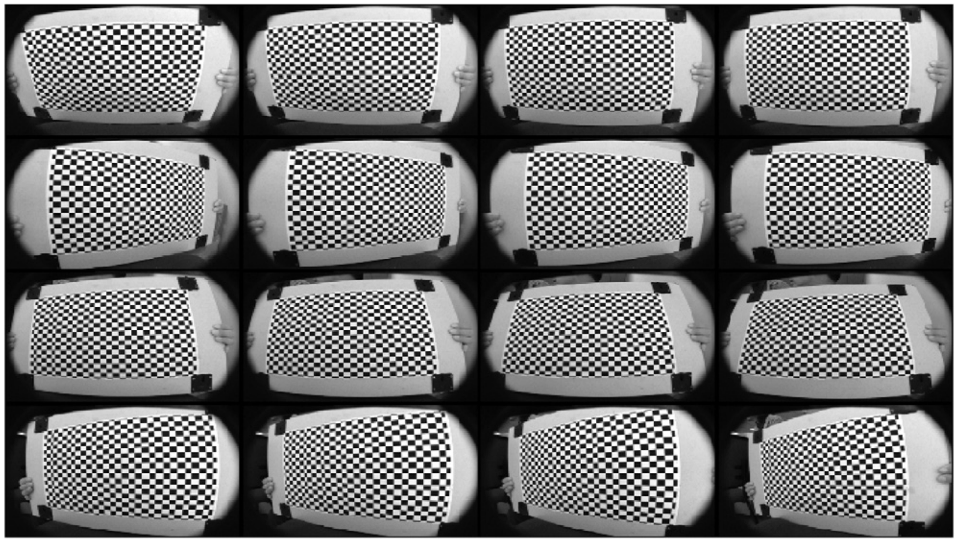

Fig. 3. Calibration images.

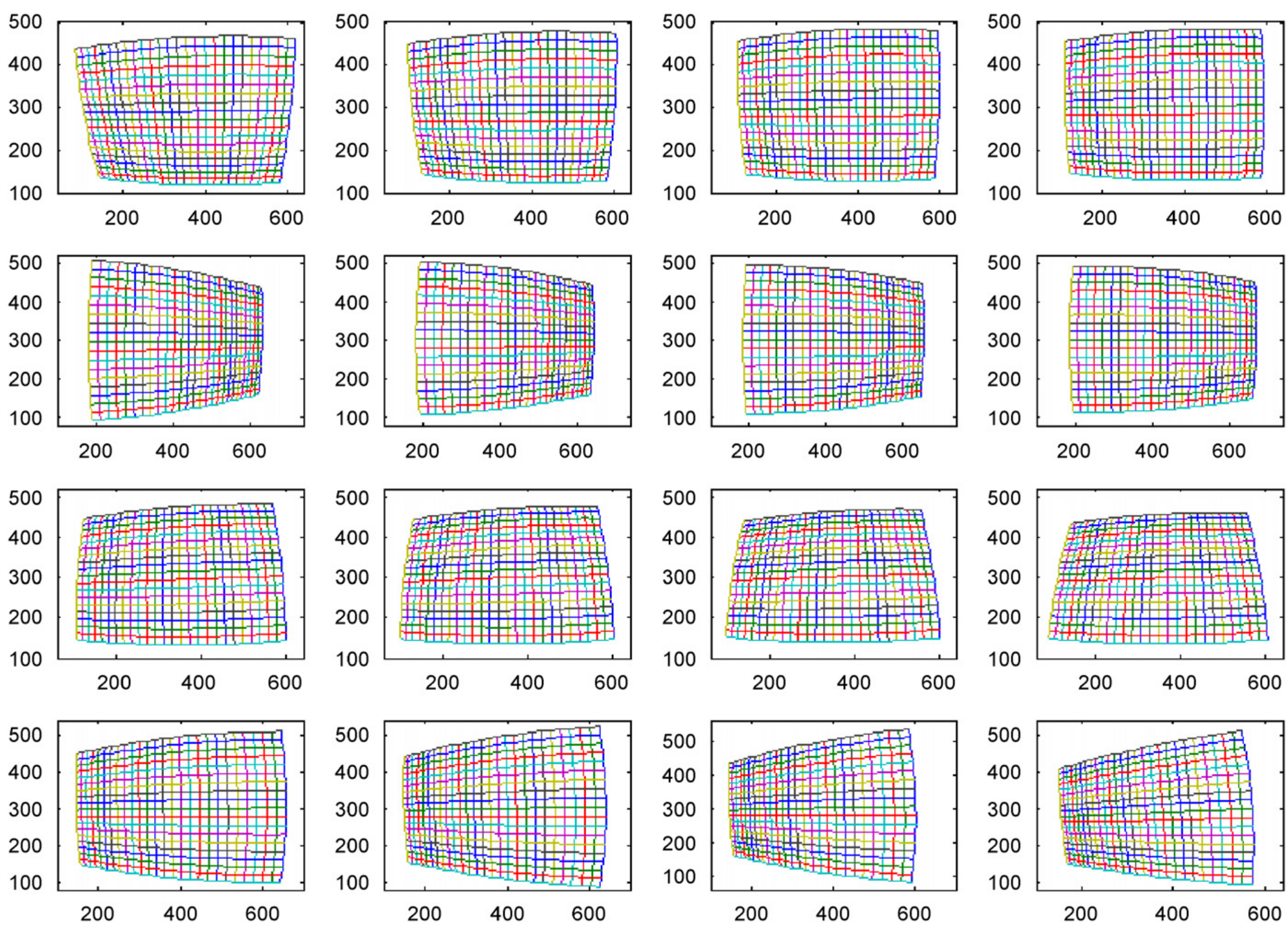

Fig. 4. Lines consist of distorted corner points.

6. Experiment results and analysis

To verify the new model, we experiment with WAT 902B CCD cameras and four types of standard CCTV lenses with focal length of 4, 6, 8, and 16 mm, respectively. According to the specification supplied by its manufacturer, the camera has a resolution of 768 × 576, with unit cell size of CCD sensor being 8.6 μm × 8.3 μm.

Table 1
Calibration results of lenses with different focal length

	Method one				Method two			
	Model I	Model II	Model III	Model IV	Model I	Model II	Model III	Model IV
Lens with 4 mm focal length (initial distortion measure $\Sigma Re_0 = 43\,430$, $\Sigma\xi_{s_0} = 22.9012$)								
u_0	373.6732	374.2665	373.5196	374.2909	374.2388	374.2740	373.7296	373.5654
v_0	285.1622	285.3049	285.3632	285.3018	285.4567	285.4398	285.5299	285.0945
$k_1(10^{-7})$	−9.7612	−12.215	−12.158	−12.146	14.342	13.700	13.413	13.472
$k_2(10^{-13})$		20.098	20.451	20.352		8.8088	9.6266	9.1502
θ(deg)			0.4297				0.4377	
ψ(deg)			1.0049				1.0794	
$p_1(10^{-12})$				0.4923				0.3554
$p_2(10^{-12})$				−0.2929				−0.4223
$q_1(10^{-12})$				0.1598				0.0227
$q_2(10^{-12})$				0.1412				−0.2037
ΣRe or $\Sigma\xi s$	4802.8	1486.0	1292.4	1313.3	1.3138	1.2085	1.1567	1.1749
Runtime (s)	4.5	5.4	7.6	9.2	3.5	4.0	4.8	5.4
Lens with 6 mm focal length (initial distortion measure $\Sigma Re_0 = 29\,544$, $\Sigma\xi s_0 = 15.2574$)								
u_0	353.8857	353.6051	353.2901	353.6363	352.7168	353.3112	353.4427	353.4427
v_0	255.8465	256.0880	256.2937	256.1030	256.6656	256.4621	256.4734	256.4734
$k_1(10^{-7})$	−6.2882	−7.0898	−7.0333	−6.9907	8.1626	7.331	7.0573	7.1315
$k_2(10^{-13})$		5.3947	5.6996	5.4005		9.5209	9.7097	9.0216
θ(deg)			0.6716				0.6623	
ψ(deg)			0.5624				0.5489	
$p_1(10^{-12})$				0.4286				−0.2217
$p_2(10^{-12})$				0.4162				−0.3169
$q_1(10^{-12})$				0.4490				−0.3724
$q_2(10^{-12})$				0.4631				−0.4883
ΣRe or $\Sigma\xi s$	1920.5	1381.4	1238.3	1244.0	2.1117	1.9525	1.8785	1.8801
Runtime(s)	4.5	5.4	7.6	9.2	3.5	4.0	4.8	5.4
Lens with 8 mm focal length (initial distortion measure $\Sigma Re_0 = 28\,363$, $\Sigma\xi s_0 = 15.7973$)								
u_0	367.0706	365.7418	365.6448	365.9668	365.7260	366.0024	366.0866	365.0489
v_0	286.9766	286.9182	287.4309	287.3736	288.0143	287.6160	287.9597	287.5534
$k_1(10^{-7})$	−6.8764	−7.4874	−7.6564	−7.6645	9.0296	7.8327	7.7710	7.7850
$k_2(10^{-13})$		5.7645	6.288	6.3826		11.231	11.517	11.593
θ(deg)			2.6566				2.6853	
ψ(deg)			1.0804				1.0587	
$p_1(10^{-12})$				−0.3535				−0.0085
$p_2(10^{-12})$				−0.4672				−0.2738
$q_1(10^{-12})$				−0.3513				−0.2716
$q_2(10^{-12})$				−0.3822				−0.0246
ΣRe or $\Sigma\xi s$	2017.5	1598.7	1484.3	1487.6	2.1330	1.9001	1.8955	1.8963
Runtime (s)	4.5	5.4	7.6	9.2	3.5	4.0	4.8	5.4
Lens with 16 mm focal length (initial distortion measure $\Sigma Re_0 = 9300.7$, $\Sigma\xi s_0 = 5.8309$)								
u_0	341.4156	346.8568	343.1470	344.4512	344.5401	348.8027	342.6093	348.6002
v_0	371.3192	365.7502	373.4343	372.2659	371.5485	372.1330	373.9878	372.4733
$k_1(10^{-7})$	−1.3701	−1.1311	−1.1111	−1.1206	1.5204	1.0733	1.0924	1.0486
$k_2(10^{-13})$		−1.1877	−1.1383	−1.1143		2.0915	1.7388	2.0694
θ(deg)			−0.4755				−0.4678	
ψ(deg)			2.4877				2.4037	
$p_1(10^{-12})$				−0.3668				0.0160
$p_2(10^{-12})$				−0.3735				0.2162
$q_1(10^{-12})$				−0.7710				0.0425
$q_2(10^{-12})$				−0.3502				−0.6648
ΣRe or $\Sigma\xi s$	2676.8	2633.8	2600.8	2609.7	3.5521	3.5081	3.5024	3.5030
Runtime (s)	4.5	5.4	7.6	9.2	3.5	4.0	4.8	5.4

For each lens, 16 images of a checkerboard at different poses and positions are taken as shown in Fig. 3, which are from a camera with focal length of 4 mm. Corner points in each image are extracted by Harris corner finder method [20], forming 19 approximately horizontal lines and 27 approximately vertical lines as shown in Fig. 4, which are from the images in Fig. 3.

For each type with focal length of 4, 6, 8, and 16 mm, respectively, at least three lenses have been tested, and the results

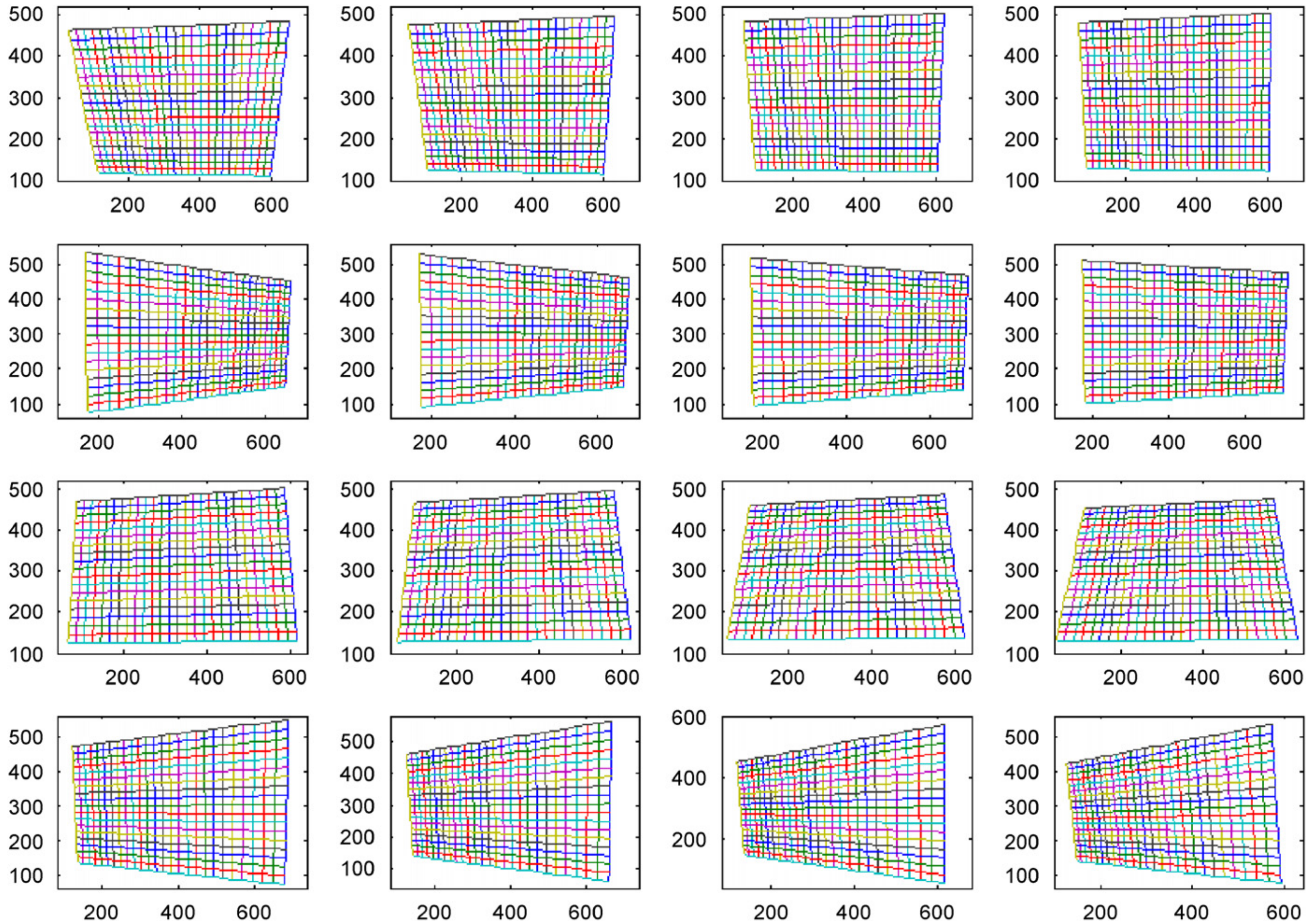

Fig. 5. Lines consist of corner points corrected by model III.

are consistent with one another on the whole. Due to the limit of pages, just a typical result of each type is listed in Table 1, where the Runtime is based on the computer configured with Pentium IV 1.7 G CPU, 256 M DDR and Matlab 6.5.

In terms of correcting effect upon lens distortion, Table 1 shows that models III and IV are about the same, and both of them are better than model II, which is better than model I in turn. Because of having more parameters, it is natural that models III and IV are better than model II, and model II is better than model I. Although model IV has more parameters than model III, it has about the same effect upon distortion as model III. The reason lies in that the parameters in model IV are not independent from one another physically, as discussed in Section 3. In addition, more parameters increase the possibility to converge to local minima. On the contrary, model III decouples the parameters physically and keeps the necessary independent parameters. Fewer parameters are beneficial to avoid converging to local minima. Consequently, model III has about the same correcting effect upon lens distortion as model IV.

In terms of runtime, Table 1 shows that the more parameters a model has, the longer it will take. Compared with model IV, model III can reduce runtime by about 20%. In addition, the runtime by method two is less than that by method one, because method two needs no straight-line fitting.

It can be seen from Table 1 that the calibration results from methods one and two are consistent with each other. The center of distortion, pitch angle θ and yaw angle ψ obtained from different methods are approximately equal to each other. Of course, the radial and tangential distortion coefficients are different in results from different methods, because their meanings are different in different methods. Distortion models are expressed in inverse formulas by methods one and method two, as discussed in Section 2.

It can also be seen from Table 1 that the shorter the focal length of a lens is, the larger its distortion is, and the more effective the model III is. For lenses with focal length of 4, 6 and 8 mm, model III can reduce the sum of residues by about 10% compared with model II. Fig. 5 shows the corrected results of lines in Fig. 4 by model III with parameters from method one, where the average residue of each corner point to the fitted straight line it belongs to is about 0.08 pixels.

Fig. 6 further shows correcting effects of different models and methods upon lens distortion. It can be seen from Fig. 6 that difference among effects of different models decreases as the focal length of a lens increases. For lenses with focal length of 4, 6 and 8 mm, difference among correcting effects of different models upon distortion are obvious. Figs. (a_1), (b_1), (a_2), (b_2), (a_3) and (b_3) of Fig. 6 show that model I is not enough to

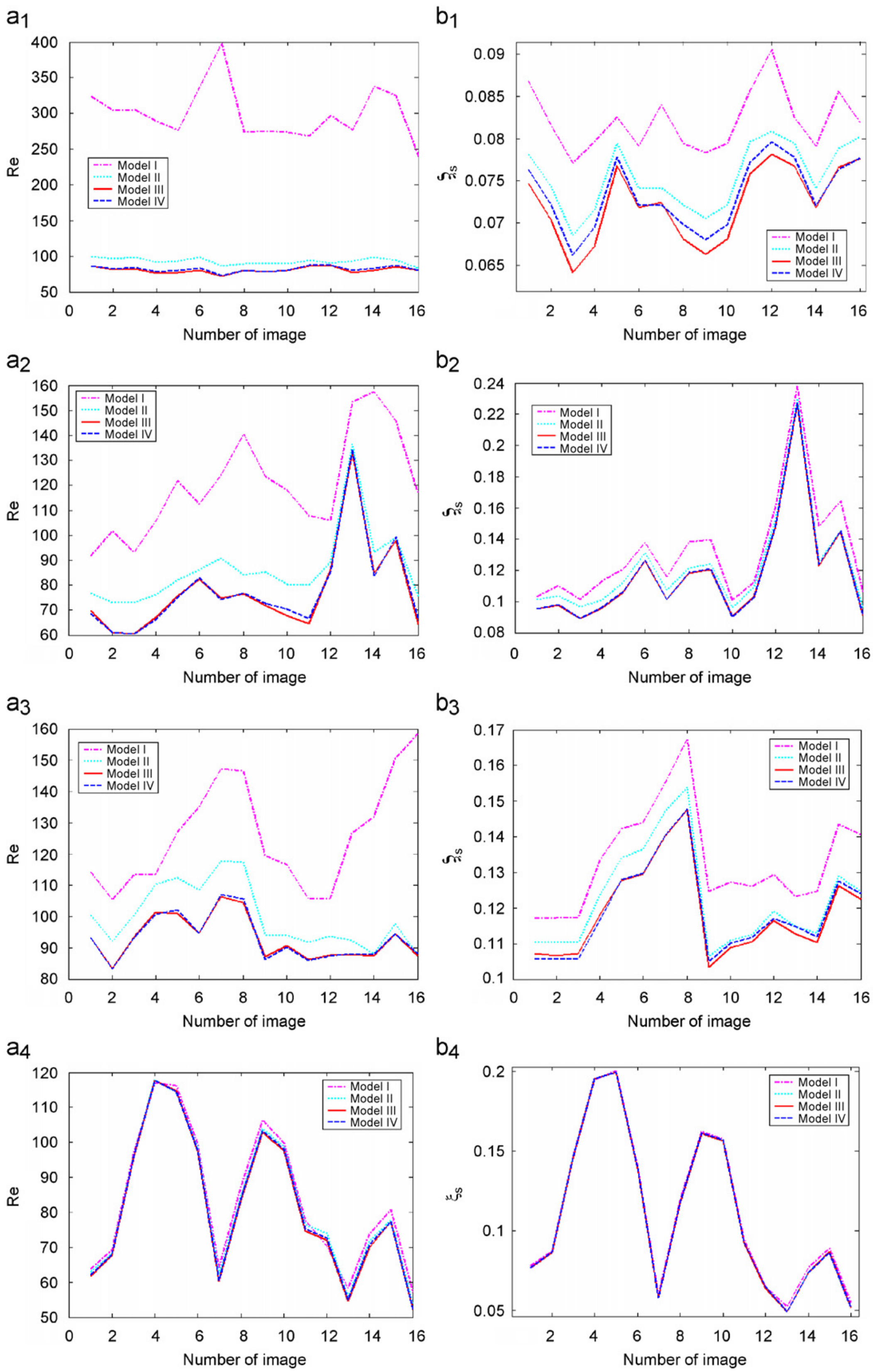

Fig. 6. Correcting effects of different models upon distortion. (a_1) $f = 4$ mm, by method one; (b_1) $f = 4$ mm, by method two; (a_2) $f = 6$ mm, by method one; (b_2) $f = 6$ mm, by method two; (a_3) $f = 8$ mm, by method one; (b_3) $f = 8$ mm, by method two; (a_4) $f = 16$ mm, by method one; (b_4) $f = 16$ mm, by method two.

correct distortion of lenses with focal length of less than 8 mm. For such lenses, model II, model III or model IV has to be used when good correcting effect is desired. In addition, it can also be seen that models III and IV are better than model II, which demonstrates that the tangential distortion should be taken into account for lenses with short focal length.

To sum up, the new model has about the same correcting effect upon distortion as the conventional model, though it has fewer parameters than the conventional model. In addition, the new model has more explicit physical meaning, which can tell us where the distortion comes from, and can indicate a direction to remove or reduce lens distortion. The new model has been used to calibrate the vision system of our surgical robot and got the benefits of improving calibration accuracy by about 10% compared with the calibration result from model II, and reducing runtime by about 20% compared with model IV.

7. Conclusion and discussion

In this paper, a new calibration model of camera lens distortion is proposed. The new model expresses lens distortion as radial distortion plus a transform from ideal image plane to real sensor array plane. The transform is determined by two angular parameters describing the pose of the real sensor array plane with respect to the ideal image plane and two linear parameters locating the real sensor array with respect to the optical axis. Experiments show that the new model has about the same correcting effect upon lens distortion as the conventional model including all the radial distortion, decentring distortion and prism distortion.

Compared with the conventional model, the new model has fewer parameters to be calibrated and more explicit physical meaning. The fewer parameters cannot only simplify the calibrating process, but also reduce the possibility to get local minima. The explicit physical meaning tells us where the distortion comes from, which can indicate a direction for manufacturer to remove or reduce lens distortion.

Acknowledgements

This research is supported by the National Natural Science Foundation of China (No. 60675017) and the National Basic Research Program (973) of China (No. 2006CB303103).

References

[1] D.C. Brown, Close-range camera calibration, Photogramm. Eng. 37 (8) (1971) 855–866.
[2] W. Faig, Calibration of close-range photogrammetry systems: mathematical formulation, Photogramm. Eng. Remote Sensing 41 (12) (1975) 1479–1486.
[3] R.Y. Tsai, A versatile camera calibration technique for high-accuracy 3D machine vision metrology using off-the-shelf TV cameras and lenses, IEEE J. Robotics Automat. 3 (4) (1987) 323–344.
[4] B. Caprile, V. Torre, Using vanishing points for camera calibration, Int. J. Comput. Vision 4 (2) (1990) 127–140.
[5] J. Weng, P. Cohen, M. Herniou, Camera calibration with distortion models and accuracy evaluation, IEEE Trans. Pattern Anal. Mach. Intell. 14 (10) (1992) 965–980.
[6] G.Q. Wei, S.D. Ma, A complete two-plane camera calibration method and experimental comparisons, in: Proceedings of the Fourth International Conference on Computer Vision, May 1993, pp. 439–446.
[7] R.G. Willson, S.A. Shafer, What is the center of the image? Technical Report CMU-CS-93-122, Carnegie Mellon University, 1993.
[8] T.A. Clarke, J.G. Fryer, The development of camera calibration methods and models, Photogramm. Rec. 16 (91) (1998) 51–66.
[9] Z. Zhang, A flexible new technique for camera calibration, IEEE Trans. Pattern Anal. Mach. Intell. 22 (11) (2000) 1330–1334.
[10] Z. Zhang, Camera calibration with one-dimensional objects, IEEE Trans. Pattern Anal. Mach. Intell. 26 (7) (2004) 892–899.
[11] F. Devernay, O. Faugeras, Straight lines have to be straight, Mach. Vision Appl. 13 (2001) 14–24.
[12] C. McGlone, E. Mikhail, J. Bethel, Manual of Photogrammetry, fifth ed., American Society of Photogrammetry and Remote Sensing, 2004.
[13] A. Basu, S. Licardie, Alternative models for fish-eye lenses, Pattern Recognition Lett. 16 (4) (1995) 433–441.
[14] S. Shah, J.K. Aggarwal, Intrinsic parameter calibration procedure for a (high distortion) fish-eye lens camera with distortion model and accuracy estimation, Pattern Recognition 29 (11) (1996) 1775–1778.
[15] S.S. Beauchemin, R. Bajcsy, Modeling and removing radial and tangential distortions in spherical lenses, Multi-Image Analysis, Lecture Notes in Computer Science, vol. 2032, Springer, Berlin, 2001, pp. 1–21.
[16] L. Ma, Y.Q. Chen, K.L. Moore, Flexible camera calibration using a new analytical radial undistortion formula with application to mobile robot localization, in: IEEE International Symposium on Intelligent Control, Houston, USA, October 2003.
[17] J. Mallon, P.F. Whelan, Precise radial un-distortion of images, in: Proceedings of the 17th International Conference on Pattern Recognition (ICPR' 2004).
[18] P.F. Sturm, S. Ramalingam, A generic concept for camera calibration, in: Proceedings of the Fifth European Conference on Computer Vision (ECCV' 2004).
[19] R.I. Hartley, S.B. Kang, Parameter-free radial distortion correction with centre of distortion estimation, in: Proceedings of the 10th International Conference on Computer Vision (ICCV 2005).
[20] J.-Y. Bouguet, Camera Calibration Toolbox for Matlab, Supplied by Computer Vision Research Group, Department of Electrical Engineering, California Institute of Technology.
[21] B. Prescott, G.F. McLean, Line-based correction of radial lens distortion, Graphical Models Image Process. 59 (1) (1997) 39–47.
[22] M. Ahmed, A. Farag, Nonmetric calibration of camera lens distortion: differential methods and robust estimation, IEEE Trans. Image Process. 14 (8) (2005).

About the Author—JIANHUA WANG received the BS degree in automatic control from Beijing University of Aeronautics & Astronautics, China, the MS degree in pattern recognition and intelligent system from Chongqing University, China, and now is a PhD candidate in pattern recognition and intelligent system of Shanghai Jiao Tong University, China. His research interests include 3D computer vision, intelligent system and robot.

About the Author—YUNCAI LIU received the PhD degree from the University of Illinois at Urbana-Champaign, in the Department of Electrical and Computer Science Engineering, in 1990, and worked as an associate researcher at the Beckman Institute of Science and Technology from 1990 to 1991. Since 1991, he had been a system consultant and then a chief consultant of research in Sumitomo Electric Industries, Ltd., Japan. In October 2000, he joined the Shanghai Jiao Tong University as a distinguished professor. His research interests are in image processing and computer vision, especially in motion estimation, feature detection and matching, and image registration. He also made many progresses in the research of intelligent transportation systems.